SUPPLEMENTARY INFORMATION

Supplementary Discussion

The cell cycle machinery and the DNA damage response network are highly interconnected and co-regulated in assuring faithful duplication and partition of genetic materials into two daughter cells. The impeccable communication between these two essential biological processes in part relies on shared key cellular factors such as CDC25 and ATR. Here, our studies also position MLL at this critical interface. MLL directly regulates the expression of *Cyclins* and thus facilitates a normal G1/S transition[1-2], whereas upon DNA damage MLL accumulates and functions as a key ATR signaling effector to delay replication for repair. Since ATM is required for the activation of ATR in response to γ-IR[3], ATM may indirectly signal MLL accumulation, which is supported by the observation that double deficiency of ATM and ATR was required to completely abrogate DNA damage induced MLL accumulation (Fig. 2c).

The MLL biology is complex: MLL orchestrates cell fate, cell cycle, stem cell and checkpoint, and its activity can be modulated by post-translational modifications including phosphorylation, degradation and site-specific proteolysis[4-5]. These unique properties underscore the perplexing pathophysiology underlying MLL leukemias. MLL-fusions act as gain-of-function mutants in *HOX* gene expression[4-7], whereas they function as dominant-negative mutants in the S phase checkpoint response by preventing the ATR-mediated phosphorylation and stabilization of wild-type MLL. Altogether, a multifaceted attack on cellular integrity is initiated upon chromosome translocations that disrupt MLL, likely explaining the aggressive clinical features associated with MLL leukemias[8].

Supplementary Figures.

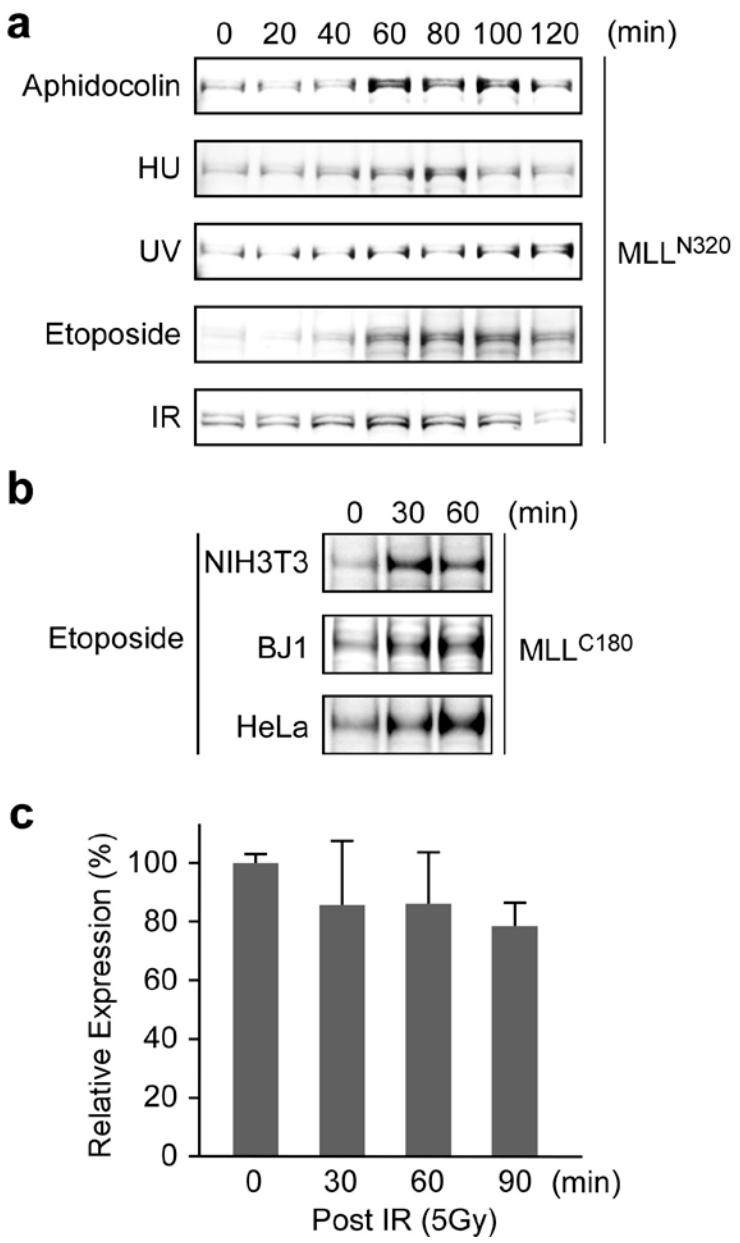

Supplementary Figure 1. DNA damage induces MLL. a, 293T cells were treated with the indicated DNA insults for the indicated times and subjected to anti-N terminus MLL (MLL^{N320}) Western blot analyses. **b,** NIH3T3, hTERT-BJ1, and HeLa cells were treated with 25μM etoposide for the indicated times and the levels of MLL were detected with anti-MLL^{C180} antibody. **c,** Synchronized mid-S phase 293T cells were treated with 5 Gy of γ-IR and qRT-PCR analysis was performed on mRNA purified at the indicated times post-treatment. Data shown are mean ± s.d. of three independent experiments. Western blot signals were quantified and presented in Supplementary Fig. 13.

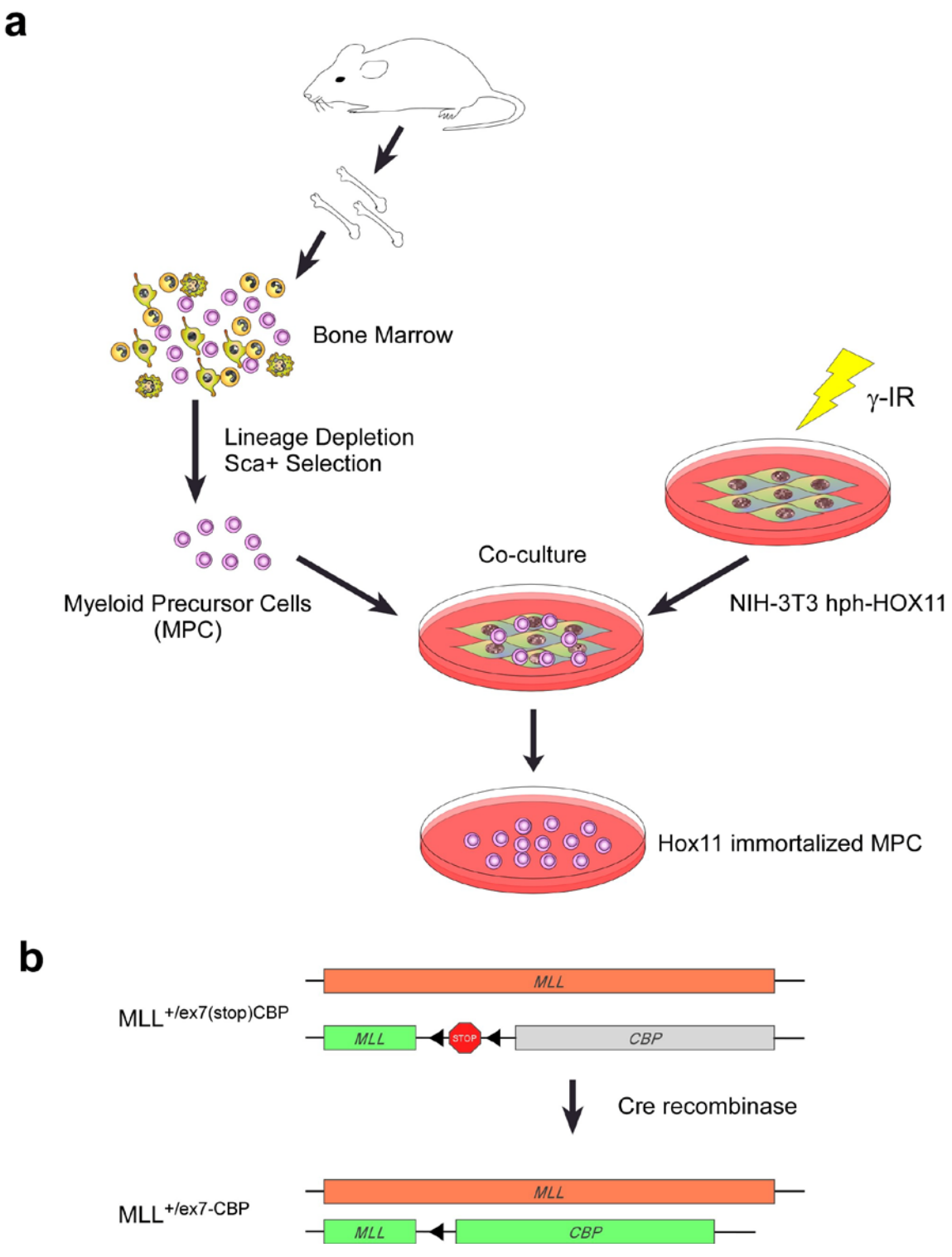

Supplementary Figure 2. Schematic diagram of the generation of *MLL*$^{+/ex7(stop)CBP}$ and *MLL*$^{+/ex7-CBP}$ Myeloid Precursor Cells.

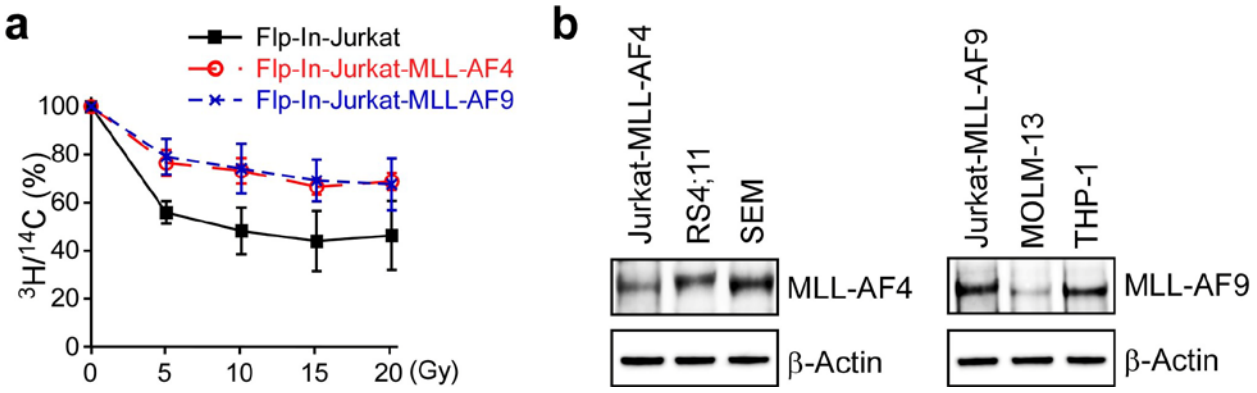

Supplementary Figure 3. Flp-In Jurkat cells carrying MLL-fusions exhibit an RDS phenotype. a, Flp-In Jurkat vector control, Flp-In Jurkat MLL-AF4, and Flp-In Jurkat MLL-AF9 cells were treated with the indicated doses of γ-IR and the incorporation of ^3H thymidine and ^{14}C thymidine was analyzed. Data shown are mean ± s.d. of three independent experiments. **b**, The expression of MLL-AF4 and MLL-AF9 in Flp-In Jurkat cells was compared to the existing human MLL leukemia cell lines.

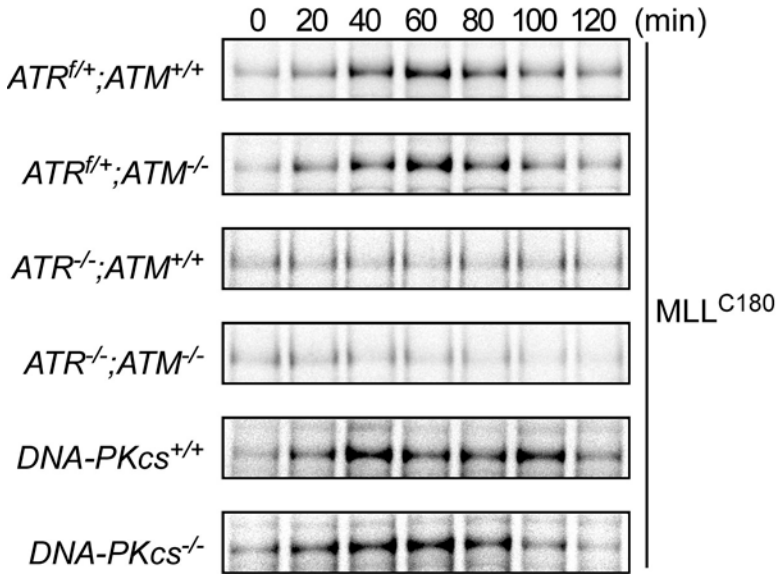

Supplementary Figure 4. ATR is the principal proximal kinase required for the MLL accumulation upon DNA insults. MEFs of the indicated genotypes were treated with 25 μM etoposide for the indicated times and subjected to anti-MLL immunoblot analyses. Western blot signals were quantified and presented in Supplementary Fig. 13.

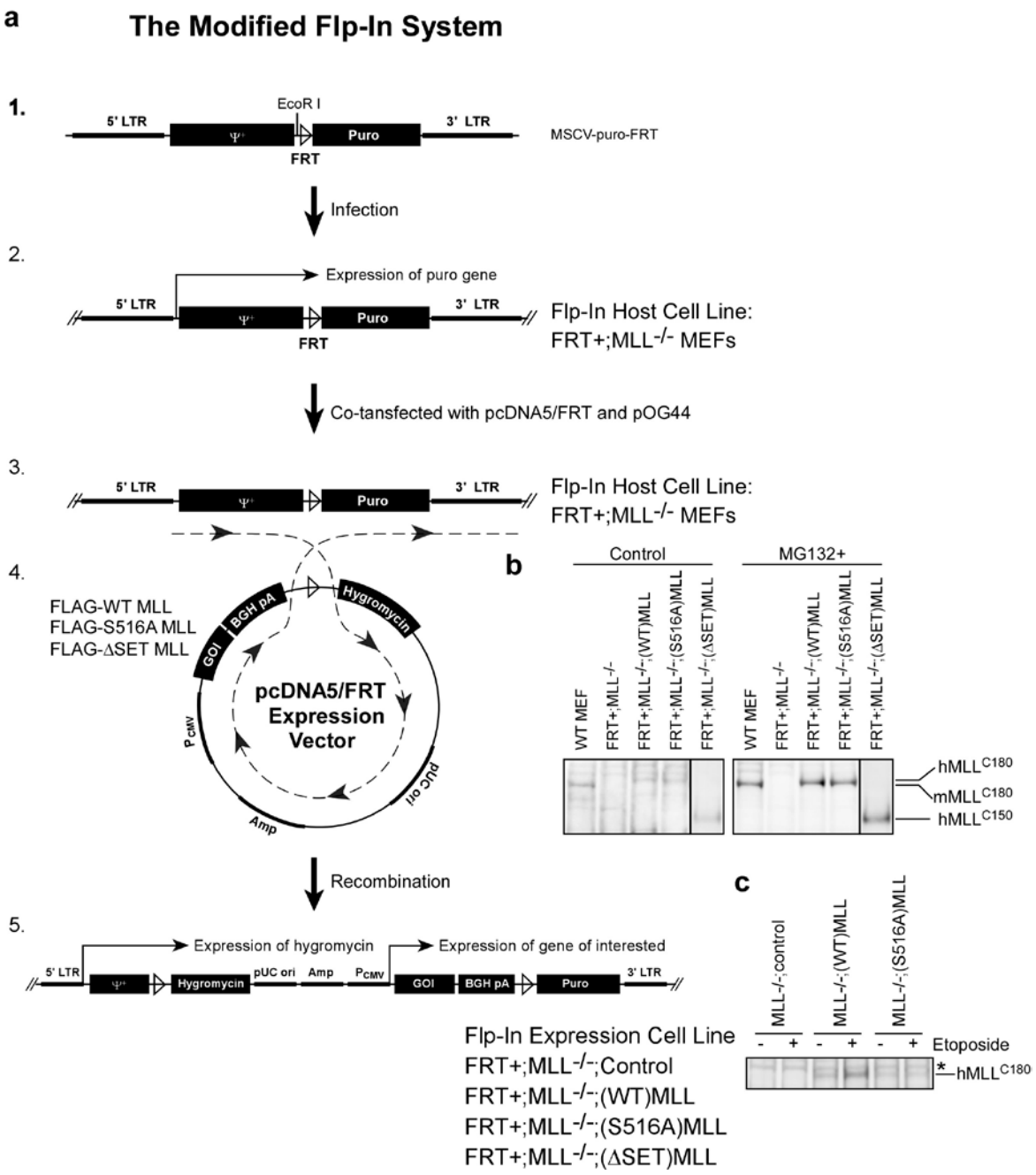

Supplementary Figure 5. The generation of *FRT+;MLL$^{-/-}$;control, FRT+;MLL$^{-/-}$;(WT)MLL, FRT+;MLL$^{-/-}$;(S516A)MLL* and *FRT+;MLL$^{-/-}$;(ΔSET)MLL* MEFs. **a**, Schematic diagram depicts our modified Flp-In system. **b**, The expression of WT and S516A mutant human MLL in reconstituted *MLL$^{-/-}$* MEFs was determined by anti-MLL immunoblots. hMLL and mMLL denote human and mouse MLL, respectively. **c**, The indicated MEFs were synchronized at S phase, treated with etoposide, and subjected to anti-MLL Western blot analysis. The residual activity of MLL(S516A) observed in Fig. 3d could be due to its low, remaining expression during DNA damage. Asterisk denotes cross-reactive bands.

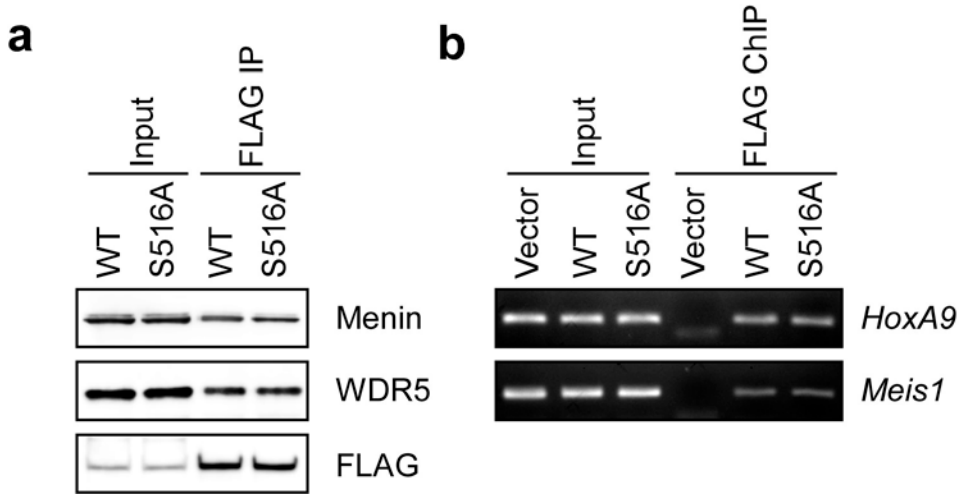

Supplementary Figure 6. The S516A mutant MLL forms stable complexes with WDR5 and Menin, and targets to the HoxA9 and Meis1 promoters as wild-type MLL. a, 293T cells were transfected with FLAG tagged wild-type and S516A mutant MLL and subjected to anti-FLAG immunoprecipitation assays. The co-precipitated Menin and WDR5 were determined by Western blots. **b**, *MLL*$^{-/-}$ MEFs reconstituted with FLAG-WT MLL or FLAG-S516A MLL (Supplementary Fig. 5) were subjected to ChIP assays using anti-FLAG antibody and co-precipitated DNA was analyzed with *HoxA9* and *Meis1* promoter-specific primers.

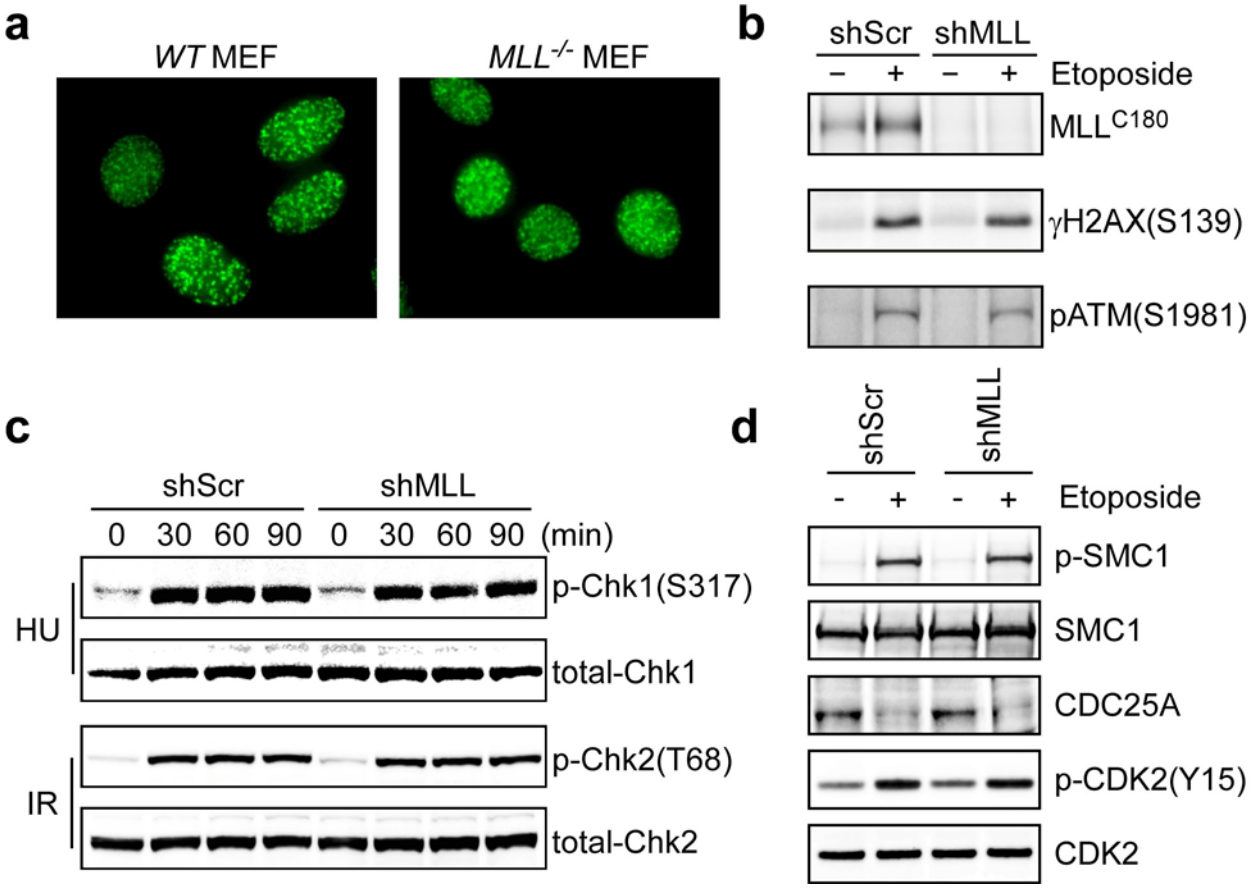

Supplementary Figure 7. Deficiency in MLL does not affect the upstream DNA damage signaling. a, Wild-type or *MLL*$^{-/-}$ MEFs were treated with 25 μM etoposide for 10 minutes and subjected to anti-γH2AX immunofluorescence assays. **b,** Deficiency in MLL does not affect the serine 139 and the serine 1981 phosphorylation of H2AX and ATM, respectively. 293T cells with scramble- or MLL-shRNA knockdown were treated with 25 μM etoposide for 15 minutes and subjected to Western blot analyses using the indicated antibodies. **c,** 293T cells with scramble- or MLL-shRNA were treated with 1 mM HU for the indicated times and subjected to anti-phospho-serine 317 Chk1 and anti-Chk1 Western blot analyses (upper panel). 293T cells with scramble- or MLL-shRNA knockdown were treated with 5 Gy of γ-IR, harvested at the indicated times post-treatment, and subjected to anti-phospho-threonine 68 Chk2 and anti-Chk2 Western blot analyses (lower panel). **d**, Deficiency in MLL does not affect the serine 966 phosphorylation of SMC1, the degradation of CDC25A, and the enhanced Y15 phosphorylation of CDK2 upon DNA damage. 293T cells with the indicated knockdown were treated with etoposide and subjected to Western blot analyses using the indicated antibodies.

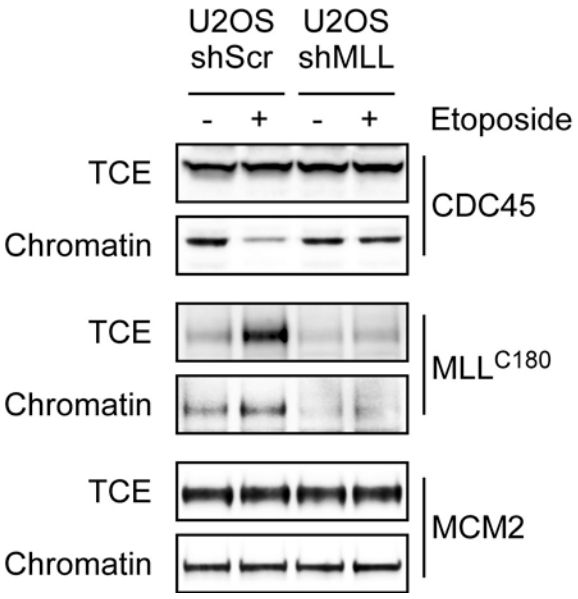

Supplementary Figure 8. MLL is required to prevent chromatin association of CDC45 upon DNA damage in U2OS cells. The chromatin association of CDC45, MLL, and MCM2 upon DNA damage in control- or MLL-knockdown cells was examined. TCE denotes total cell extracts and chromatin denotes chromatin-bound fractions. U2OS cells were synchronized in S phase, treated with 25 μM etoposide for 90 minutes, fractionated and subjected to Western blot analyses using the indicated antibodies.

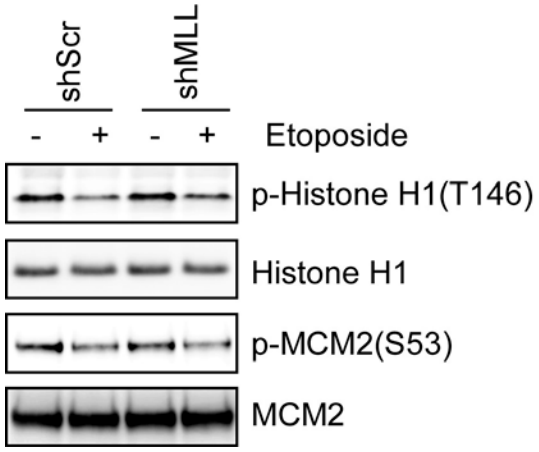

Supplementary Figure 9. Deficiency of MLL does not affect the threonine 146 phosphorylation of histone H1 by CDK2 and the serine 53 phosphorylation of MCM2 by DDK. 293T cells with scramble- or MLL-shRNA knockdown were treated with 25 μM etoposide for 90 minutes and subjected to Western blot analyses with the indicated antibodies.

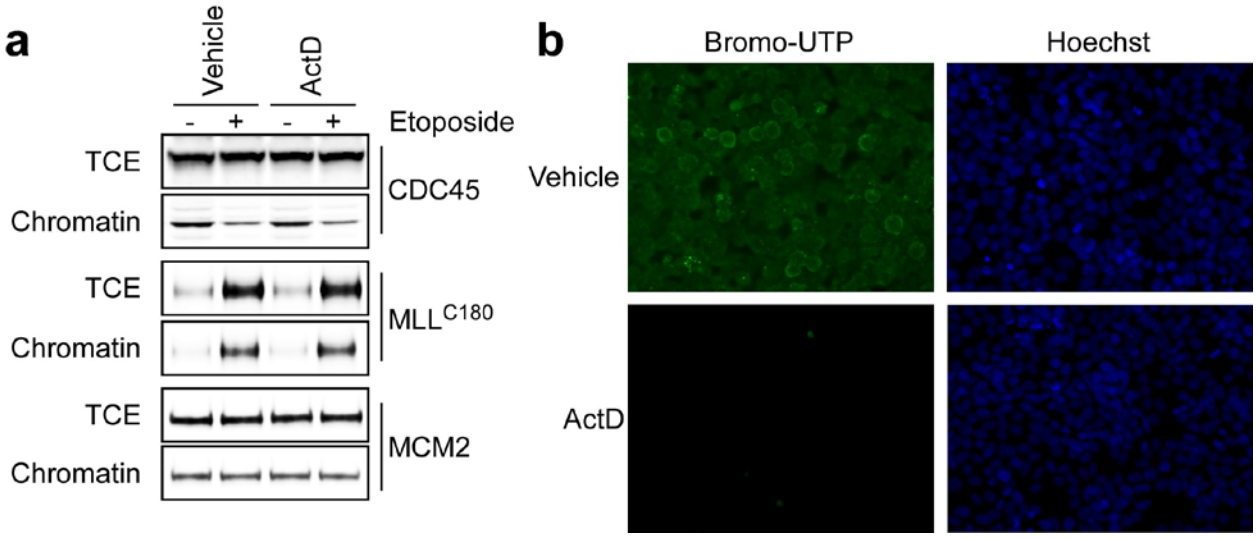

Supplementary Figure 10. The MLL-mediated inhibition of CDC45 loading during the S phase checkpoint activation is transcription-independent. a, The chromatin association of CDC45, MLL, and MCM2 upon DNA damage in 293T cells was examined in the presence of 1 μM actinomycin-D that inhibits transcription. 293T cells were treated with 1 μM actinomycin-D for 30 minutes and then treated with 25 μM etoposide for the indicated times before subjected to fractionations and Western blot analyses using the indicated antibodies. TCE denotes total cell extracts and chromatin denotes chromatin-bound fractions. **b**, 293T cells were pretreated with vehicle or actinomycin-D for 30 minutes, transfected with BrUTP for 2 hours, and then subjected to immunostain analyses. Green signals indicate active transcription. Hoechst stains for nucleus.

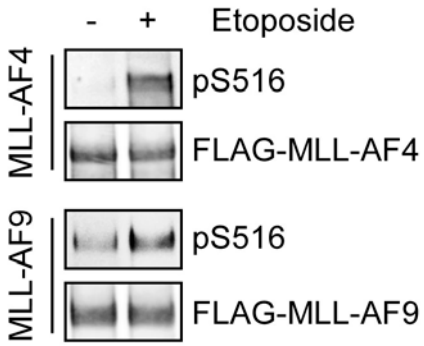

Supplementary Figure 11. MLL-AF4 and MLL-AF9 are phosphorylated at serine 516 upon DNA damage. 293T cells were transfected with FLAG-MLL-AF4 and FLAG-MLL-AF9, treated with etoposide for 90 minutes, subjected to anti-FLAG immunoprecipitation assays, and detected by anti-phospho-MLL(S516) and anti-FLAG antibodies.

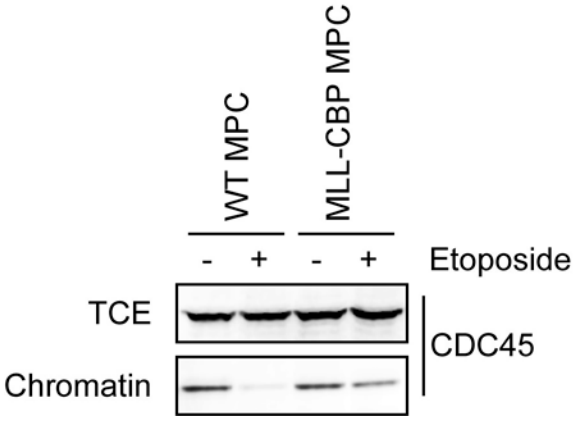

Supplementary Figure 12. The *MLL*$^{+/ex7\text{-}CBP}$ MPCs exhibit aberrant CDC45 loading upon DNA damage. Wild-type and *MLL*$^{+/ex7\text{-}CBP}$ MPCs were treated with etoposide for 90 minutes, fractionated, and subjected to anti-CDC45 immunoblot analyses.

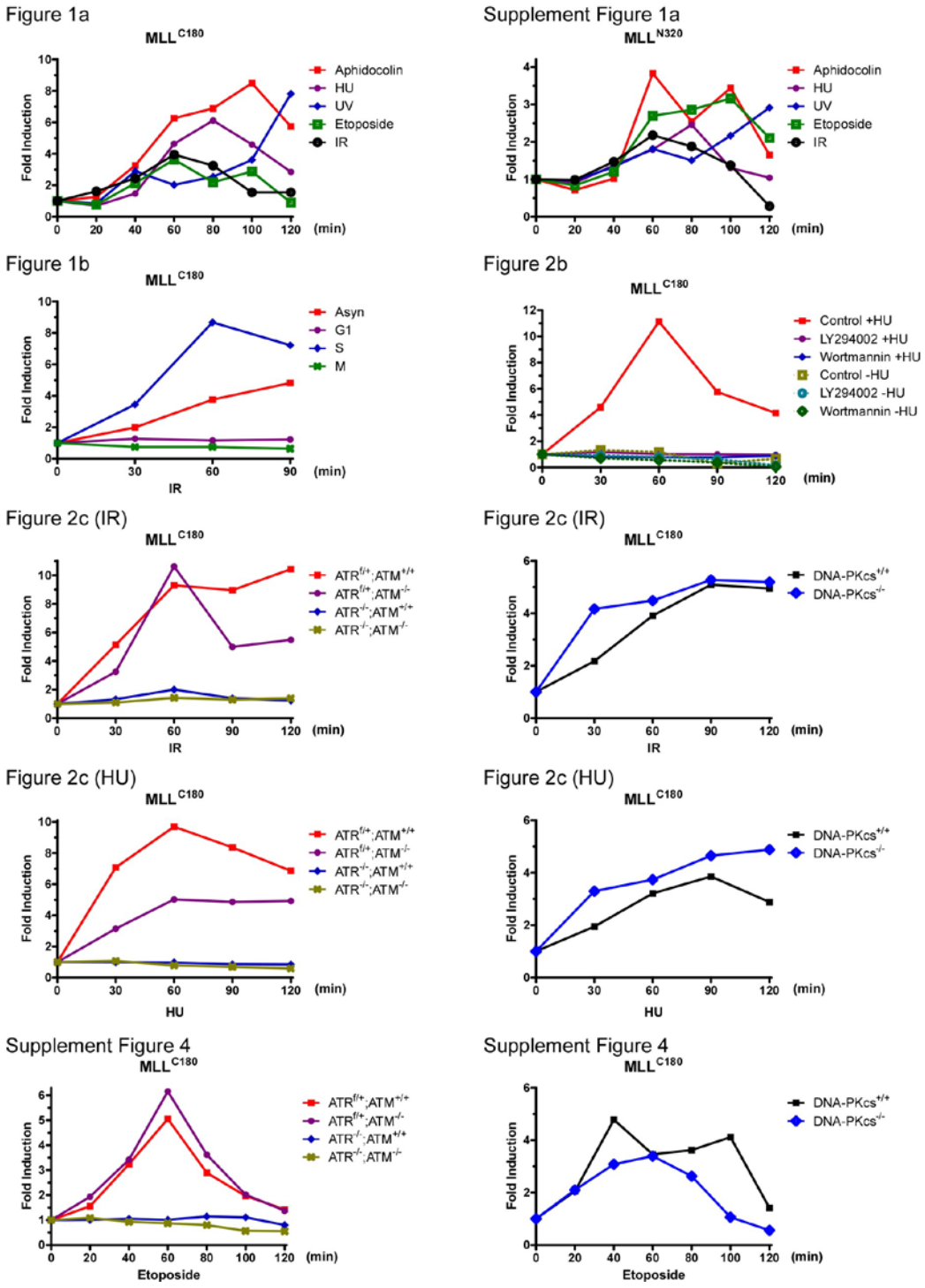

Supplementary Figure 13. Quantification of immunoblots presented in Fig. 1, 2, and Supplementary Fig. 1, 4. Western blot signals were acquired with the LAS-3000 Imaging system (FujiFilm) and then analyzed by ImageGauge software (FujiFilm). The signals at time 0 were assigned as 1.

References:

1 Takeda, S. *et al.* Proteolysis of MLL family proteins is essential for taspase1-orchestrated cell cycle progression. *Genes Dev* **20**, 2397-2409 (2006).

2 Liu, H., Cheng, E. H. & Hsieh, J. J. Bimodal degradation of MLL by SCFSkp2 and APCCdc20 assures cell cycle execution: a critical regulatory circuit lost in leukemogenic MLL fusions. *Genes Dev* **21**, 2385-2398 (2007).

3 Jazayeri, A. *et al.* ATM- and cell cycle-dependent regulation of ATR in response to DNA double-strand breaks. *Nat Cell Biol* **8**, 37-45 (2006).

4 Krivtsov, A. V. & Armstrong, S. A. MLL translocations, histone modifications and leukaemia stem-cell development. *Nature reviews cancer* **7**, 823-833 (2007).

5 Liu, H., Cheng, E. H. & Hsieh, J. J. MLL fusions: pathways to leukemia. *Cancer biology & therapy* **8**, 1204-1211 (2009).

6 Rodriguez-Perales, S., Cano, F., Lobato, M. N. & Rabbitts, T. H. MLL gene fusions in human leukaemias: in vivo modelling to recapitulate these primary tumourigenic events. *International journal of hematology* **87**, 3-9 (2008).

7 Meyer, C. *et al.* New insights to the MLL recombinome of acute leukemias. *Leukemia* **23**, 1490-1499 (2009).

8 Zuber, J. *et al.* Mouse models of human AML accurately predict chemotherapy response. *Genes Dev* **23**, 877-889 (2009).